HHS Public Access

Author manuscript

Brain Stimul. Author manuscript; available in PMC 2016 May 01.

Published in final edited form as:

Brain Stimul. 2015 ; 8(3): 624–636. doi:10.1016/j.brs.2014.11.018.

Non-invasive access to the vagus nerve central projections via electrical stimulation of the external ear: fMRI evidence in humans

Eleni Frangos[a], **Jens Ellrich**[b,c,d], and **Barry R. Komisaruk**[a]

Eleni Frangos: frangos.eleni@gmail.com; Jens Ellrich: ellrichj@gmail.com; Barry R. Komisaruk: brk@psychology.rutgers.edu

[a]Department of Psychology, Rutgers University, 101 Warren St, Newark, NJ 07102

[b]Cerbomed GmbH, Henkestrasse 91, 91052 Erlangen, Germany

[c]Department of Health Science, and Technology, Aalborg University, Fredrik Bajers Vej 7D2, DK-9220 Aalborg, Denmark

[d]Institute of Physiology and Pathophysiology, Friedrich-Alexander-University Erlangen-Nuremberg, Universitaetsstrasse 17, D-91054 Erlangen, Germany

Abstract

Background—Tract-tracing studies in cats and rats demonstrated that the auricular branch of the vagus nerve (ABVN) projects to the nucleus tractus solitarii (NTS); it has remained unclear as to whether or not the ABVN projects to the NTS in humans.

Objective—To ascertain whether non-invasive electrical stimulation of the cymba conchae, a region of the external ear exclusively innervated by the ABVN, activates the NTS and the "classical" central vagal projections in humans.

Methods—Twelve healthy adults underwent two fMRI scans in the same session. Electrical stimulation (continuous 0.25ms pulses, 25Hz) was applied to the earlobe (control, scan #1) and left cymba conchae (scan #2). Statistical analyses were performed with FSL. Two region-of-interest analyses were performed to test the effects of cymba conchae stimulation (compared to

Corresponding Author: Eleni Frangos, Department of Psychology, Rutgers University, 101 Warren Street, Room 304, Newark, NJ 07102. frangos.eleni@gmail.com, Tel: +1-201-233-7982.

Financial Disclosures: This study was supported by Cerbomed, GmbH (Erlangen, Germany) and by the National Institutes of Health Grant 2R25 GM 060826.

Conflict of Interest: Funding for this research (e.g., fMRI scan costs and honoraria to research participants) was provided by a grant from Cerbomed, GmbH, Erlangen, Germany. Cerbomed, the manufacturer of the ear stimulator, provided the instruments for this study. JE was the Chief Medical Officer of Cerbomed during the early part of this study; he is no longer affiliated with the company. BRK is a paid consultant and member of the Advisory Board of Cerbomed. EF received financial compensation from Cerbomed to support the fMRI data analysis. No contractual relations or proprietary considerations exist that restrict the dissemination of our findings.

baseline and control, earlobe, stimulation) on the central vagal projections (corrected; brainstem $p<0.01$, forebrain $p<0.05$), followed by a whole-brain analysis (corrected, $p< 0.05$).

Results—Cymba conchae stimulation, compared to earlobe (control) stimulation, produced significant activation of the "classical" central vagal projections, e.g., widespread activity in the ipsilateral nucleus of the solitary tract, bilateral spinal trigeminal nucleus, dorsal raphe, locus coeruleus, and contralateral parabrachial area, amygdala, and nucleus accumbens. Bilateral activation of the paracentral lobule was also observed. Deactivations were observed bilaterally in the hippocampus and hypothalamus.

Conclusion—These findings provide evidence in humans that the central projections of the ABVN are consistent with the "classical" central vagal projections and can be accessed non-invasively via the external ear.

Keywords

nucleus of the solitary tract; vagus nerve auricular branch; non-invasive vagus stimulation; neuromodulation; t-VNS; fMRI

Introduction

The main visceral sensory nerve – the vagus – which innervates the esophagus, trachea, lungs, heart, pancreas, stomach, intestines, etc., projects to the nucleus tractus solitarii (NTS), the first central relay of vagal afferents [5,52,54]. The vagus nerve includes a sensory "auricular" branch that innervates the external ear [5,48]. The cymba conchae of the external ear (Fig. 1a) is innervated exclusively by this branch; other regions of the external ear receive afferent innervation by this branch solely, or shared with other nerves, e.g., the posterior and inferior walls of the ear canal [13,56] and the cavity of the concha [48].

To our knowledge, there is no reported evidence in humans that the auricular branch of the vagus nerve (ABVN) projects to the NTS. However, neuroanatomical and brain imaging evidence suggests that this projection is plausible in humans. A tract-tracing study using horseradish peroxidase in cats provided evidence that the ABVN projects to the NTS, the spinal trigeminal nucleus, and other sensory nuclei within the brainstem. Primary afferent terminal labeling was observed specifically in the interstitial, dorsal, dorsolateral, and commissural subnuclei of the NTS [45]. A subsequent study in rats provided further evidence of a direct projection of the ABVN to the NTS [19]. Three functional MRI (fMRI) studies in humans investigating the effects of transcutaneous vagus nerve stimulation (t-VNS) via the external ear did not report activation of the NTS, possibly because of methodological differences or because different regions of the external ear other than the cymba conchae were stimulated and were not supplied or insufficiently supplied by the ABVN [11,35,36]. However, the brain regions that were significantly affected by the stimulation in those studies are consistent with primary and higher-order central projections of the vagus nerve. Functional MRI studies of invasive vagus nerve stimulation (VNS) also reported activity within afferent vagal projection sites [6,37,38,41,44]. The regions most commonly affected by t-VNS and VNS are the insula, thalamus, amygdala, hippocampus, postcentral gyrus, nucleus accumbens, hypothalamus, and brainstem.

In addition to the above neuroanatomical and brain imaging studies, there is evidence that t-VNS produces cognitive and behavioral effects that are also produced by VNS [7,10,22,29,41,43,53,55,57,58]. Based on conventional neuroanatomy, VNS would be expected to activate the vagal projections beginning centrally at the NTS; therefore, it is likely that t-VNS, via the ABVN, would also activate the NTS.

In the present study, we used functional MRI to test the following hypothesis: non-invasive electrical stimulation of the auricular branch of the vagus nerve (t-VNS) via the cymba conchae, exclusively innervated by the ABVN, will activate the NTS and the "classical" vagal projections. Brain regions that respond to electrical stimulation of the cymba conchae were compared to regions that respond to stimulation of the control region, the earlobe. The earlobe is innervated by the greater auricular nerve, which is a composite nerve of cervical spinal nerves 2 and 3 and projects to the nucleus cuneatus in the brainstem [48]. Preliminary findings have been published in abstract form [16–18].

Materials and Methods

The study received approval from the Rutgers University Institutional Review Board, and the "Rutgers University Brain Imaging Center (RUBIC) Common Practices for fMRI" guidelines were strictly followed.

Research Participants

Twelve healthy participants (9 females and 3 males; age range 21–71 years; mean ± SD age, 32.6 ± 13.8 years) were recruited for the study by word of mouth. Each person provided written informed consent and was compensated for participating in the study. Participants underwent two structural and functional magnetic resonance imaging scans in the same session and were instructed to remain alert and awake while viewing a sequence of still images of natural scenery ("travelogue" images) during each scan.

Stimulation Procedure

Before each scan, participants were fitted with the Cerbomed NEMOS® device designed specifically for mild electrical stimulation of the cymba conchae of the external ear (Fig. 1a) via an adjustable earpiece containing two hemispheric titanium electrodes (Fig. 1d) connected to a battery-operated stimulator. The device was used to provide transcutaneous electrical stimulation of the *left* cymba conchae and the *left* earlobe (as a control). Control stimulation of the earlobe was conducted by positioning the earpiece upside down (Fig. 1b). Cymba conchae stimulation was conducted by positioning the earpiece upright, as designed to be used (Fig. 1c).

The battery-containing stimulator unit remained in the monitor room; the unshielded cable (7 meters in length) attached to the earpiece electrodes was passed through a wave-guide to the participant in the scanner. The stimulus intensity was adjusted for each of the participants as they lay supine on the scanner gurney prior to each scan. The intensity was increased from 0.1mA in 0.1mA increments until a participant reported a "tingling" sensation that was below the intensity that produced a noxious "pricking" sensation [12]. The individual stimulation intensities that were selected in this way were 0.3–0.9mA for the

control (earlobe) stimulation condition (0.58 ± 0.19 mA; mean ± SD), and 0.3–0.8mA for the cymba conchae stimulation condition (0.43 ± 0.14 mA; mean ± SD). The non-adjustable parameters of the device were continuous 0.25msec-duration monophasic square wave pulses at 25Hz. The cable was guided from the left ear down the left side of the head, across the neck, and down the right side of the body, as this positioning resulted in the minimum artifact and maximum signal-to-noise ratio in the fMRI images.

Experimental Paradigm

Scan 1 - Control—The following data were collected in a 14-min continuous scan while subjects viewed travelogue images: 2-min rest; 7-min left earlobe stimulation; and 5-min rest.

Scan 2 - Experimental—The following data were collected in a 20-min continuous scan while subjects viewed travelogue images: 2-min rest; 7-min left cymba conchae stimulation; and 11-min rest.

The control condition (scan 1) and experimental condition (scan 2) were not counterbalanced, as a carry-over effect was expected from the experimental condition. Subjects were blind as to whether the electrode orientation was for the experimental or the control condition.

fMRI Acquisition

The fMRI scans were performed at the Rutgers University Brain Imaging Center using a 3T Siemens Trio with a Siemens 12-channel head coil. For registration purposes, anatomical images were acquired using magnetization prepared rapid gradient echo (MPRAGE) sequences (176 slices in the sagittal plane using 1mm thick isotropic voxels, TR/TE = 1900/2.52ms, field of view = 256, 256 × 256 matrix, flip angle = 9 degrees; 50% distance factor). Field maps (phase and magnitude images) were collected to correct for inhomogeneity in the magnetic field and to increase accuracy of registration during the data analysis. Gradient-echo EPI sequences were acquired of the whole brain including the entire medulla oblongata (33 slices in the axial plane using 3mm isotropic voxels, TR/TE = 2000ms/30ms, interslice gap = 1.5 mm, flip angle = 90, field of view = 192, 64×64). The same parameters were used for the field maps with the exception of the flip angle (60) and TR/TE1/TE2 (400ms/5.19ms/7.65ms).

Data Analysis

All data were preprocessed and statistically analyzed using FMRIB's Software Library ("FSL", Center for Functional Magnetic Resonance Imaging of the Brain, University of Oxford, UK) version 6.00. Lower-level fMRI data processing was carried out using FMRI Expert Analysis Tool (FEAT). The following pre-processing steps were performed at the individual level: removal of skull and non-brain tissue from the anatomical, functional images, and magnitude images using Brain Extraction Tool (BET) followed by a manual approach to ensure the removal of non-brain tissue around the brainstem; motion correction using FMRIB's Linear Image Registration Tool (MCFLIRT) (motion was <0.5mm during cymba conchae and earlobe stimulation); spatial smoothing using a 5mm full-width at half-

maximum Gaussian kernel; field inhomogeneities were corrected using B0 Unwarping in FEAT; grand-mean intensity normalization; and high pass temporal filtering (Gaussian-weighted least-squares straight line fitting, with $\sigma = 420.0$s for scan 1, and $\sigma = 600.0$s for scan 2) [25–28,59]. For analysis of the brainstem, the above pre-processing analyses were carried out a second time with the exception of spatial smoothing. Spatially smoothing a data set enables the detection of larger clusters [50] such as those found within the forebrain. However, the application of spatial smoothing to smaller areas, such as those within the brainstem, decreases the detection of smaller clusters [50]. For this reason, spatial smoothing was not applied during the preprocessing procedure for the brainstem data. Incrementally increasing the spatial smoothing kernel of the brainstem data initially results in flooded regional activity with excessive false positives and eventually failure to detect any activity. Thus, we believe that for the purpose of reducing the likelihood of false positives and more accurately representing discrete activity in the brainstem, in the present analysis, we have selected to not smooth the data.

Registration of the functional images to the high-resolution anatomical images was performed using Boundary-Based Registration (BBR) [21]. A nonlinear registration of the high-resolution anatomical to the MNI152 standard space was then performed using FMRIB's Nonlinear Registration Tool [2,3].

At the individual level, explanatory variables (EVs) were created for the 7 minutes of cymba conchae stimulation, and the 11-minute post stimulation period. The same was created for the earlobe stimulation condition (1 EV for 7 minutes of earlobe stimulation, 1 EV for the 5-minute post stimulation period). The EVs were used as regressors to determine the average activity elicited by each condition. The data were thresholded at $p=0.05$ (uncorrected). The output files (contrast of parameter estimates, or "cope" files) were then used in the higher-level analysis to determine mean group effects and perform contrast analyses between the experimental and control conditions.

Three higher-level mixed-effects analyses were performed ($n=12$): two region-of-interest (ROI) analyses (brainstem, Fig. 2a, and forebrain, Fig. 2b) to specifically test the hypothesis, and a whole-brain analysis. The ROIs were selected based on the known projections of the NTS. The masks for the following ROIs were generated using Harvard-Oxford Cortical and Subcortical Structural Atlases: lower brainstem (excluding the diencephalon and the cerebellum) (Fig. 2a), and amygdala, hippocampus, insula, nucleus accumbens, and thalamus (Fig. 2b). Masks for the hypothalamus and paracentral lobule of the cerebral cortex were created manually (Fig. 2b). Mean group effects were processed for both conditions followed by a two-sampled paired t-test to identify differences between the conditions.

All higher-level analyses were corrected for multiple comparisons. The average brainstem activity (compared to baseline) and the contrast analyses (cymba conchae > earlobe, and earlobe > cymba conchae) for the brainstem were processed using a cluster-significance threshold of $p = 0.01$. The average activity within the ROIs in the forebrain (compared to baseline) during earlobe and cymba conchae stimulation was processed using a cluster-significance threshold of $p = 0.05$. An analysis specifically testing the projections of the earlobe and cymba conchae to the primary somatosensory cortex was processed using a

cluster-significance threshold of p = 0.05 and p = 0.01, respectively. All whole-brain analyses were processed with a cluster-significance threshold of p=0.05. The range of z-scores for each analysis is indicated on each figure (the lower interval indicates the cluster-forming threshold for that particular analysis).

Results

On the basis of results presented in Table 1, stimulation of the ABVN via the cymba conchae activated the NTS and other vagal projections within the brainstem and forebrain by comparison with earlobe (control) stimulation.

Cymba conchae vs. earlobe (control) and cymba conchae vs. baseline

The group brainstem analysis of the experimental condition (cymba conchae) compared to the control condition (earlobe) revealed clear activation along the length of the left side of the medulla in the region that is consistent with the location of the ipsilateral NTS (Fig. 3a). The activity extended from the midline of the lower medulla dorsolaterally to the upper medulla (Fig. 3). Activity in the region of the spinal trigeminal nucleus (STN) was observed ipsilaterally along the length of the medulla (Fig. 3). Some contralateral activity was also observed in the region of the STN. In addition, the region of the hypoglossal nucleus was activated (Fig. 3). The activity observed along the pons was consistent with the locations of the principal sensory trigeminal nucleus (more contralateral than ipsilateral), the locus coeruleus (more contralateral than ipsilateral), and the contralateral parabrachial area (Fig. 4). The activity in the midbrain was consistent with the location of the dorsal raphe nuclei, periaqueductal gray, red nuclei, and substantia nigra (Fig. 5). These regions were also activated in the analysis of cymba conchae stimulation compared to baseline, and all, except the principal spinal trigeminal nucleus, remained activated in the post-cymba conchae stimulation period (Fig. 6). The whole-brain analyses, which included spatial smoothing within the brainstem, showed widespread activations throughout the medulla, pons and midbrain, but regional specificity was not discernible.

Compared to baseline and earlobe (control) stimulation, cymba conchae stimulation produced significant activations in the following forebrain regions: bilateral activation in the insula, paracentral lobule, and anterior thalamic nuclei, and contralateral activity in the nucleus accumbens and amygdala (Fig. 7). Activation was also observed in the region of the bed nucleus of the stria terminalis, the stria terminalis proper, the fornix, and the septum. There was widespread activation throughout the primary somatosensory cortex (more contralateral than ipsilateral) consistent with the visceral area, face area, side/back of the head (which could include external ear representation), and paracentral lobule, which is the genital area of the Penfield homuncular map (Fig. 8a,c). Deactivations were found bilaterally in the hypothalamus and extensively throughout the hippocampal formation (Fig. 9). These effects were consistent with the whole-brain analyses.

Earlobe (control) vs. cymba conchae, and earlobe (control) vs. baseline

The group brainstem analysis of earlobe (control) stimulation compared to cymba conchae stimulation (i.e., earlobe > cymba conchae) revealed activation in the ventral region of the

caudal medulla (Fig. 10a). Compared to baseline, earlobe (control) stimulation produced activation in the region of the STN, nucleus cuneatus, and ventrocaudal medulla (Fig 10b). Activation of the region of the NTS was not observed in the medulla under these control conditions (Fig. 10a,b). There was no activity in the regions of the principal sensory trigeminal nucleus, locus coeruleus, parabrachial area, dorsal raphe, or periaqueductal gray in the contrast analysis (earlobe > cymba conchae) or in the analysis of earlobe stimulation compared to baseline. Specificity within the brainstem was indiscernible due to spatial smoothing in the whole-brain analyses. However, activations were found within the ventral medulla and ventral pons. There were no deactivations in the brainstem in the analyses of earlobe stimulation compared to baseline. Brainstem activity persisting beyond the stimulation period was not observed in the control, earlobe condition. Thus, the effect of this control stimulation was markedly different from that of the experimental (cymba conchae) stimulation.

Control earlobe stimulation produced activation in the contralateral insula (Fig. 11) and in the primary somatosensory cortex (more contralateral than ipsilateral) (Fig. 8b,c) consistent with the location of the face, and side/back of the head (which could include external ear representation) consistent with the Penfield homuncular map. However, this activity was not greater than that elicited by cymba conchae stimulation, as there were no significant activations found in the earlobe (control) vs. cymba conchae analysis. We found no deactivations in the forebrain produced by earlobe stimulation. These effects were consistent with the whole-brain analysis.

Time-course analysis of cymba concha stimulation

A group time-course analysis (Fig. 12) showed a gradual increase in NTS activity that peaked after cessation of cymba conchae stimulation. Other regions also showed a gradual increase in activity during stimulation. Among all brain regions, the right amygdala showed the greatest activation during stimulation, reaching a peak during the post-stimulation period. Nearly all regions became maximally active during the post-stimulation period; their activity declined gradually, persisting throughout the 11 minutes.

Discussion

The present findings provide fMRI evidence in 12 healthy adults that 7 minutes of mild, non-invasive electrical stimulation (continuous 0.25ms pulses at 25Hz, mean intensity 0.43 mA) of the ABVN via the left cymba conchae significantly affects the central projections of the vagus nerve, compared to earlobe (control) stimulation (continuous 0.25ms pulses at 25Hz, mean intensity 0.58 mA).

Neuroanatomical studies provide evidence that the sensory vagus projects to the NTS [5]. The NTS in turn projects to the following brain sites: STN, parabrachial area, locus coeruleus, dorsal raphe, periaqueductal gray, thalamus, amygdala, insula, nucleus accumbens, bed nucleus of the stria terminalis, and hypothalamus, in addition to other higher-order projections [52,54]. In the present study, each of these named brain regions was activated in response to cymba conchae (left side) stimulation, with the exception of the hypothalamus and hippocampus, both of which were deactivated.

While the present study was conducted on a healthy population and focused on elucidating the central projections of the ABVN there are reports of cognitive and behavioral effects of t-VNS and VNS, i.e., antinociception [7,29,43,58], anti-depression [22,41,53], and anti-convulsion [10,55,57]. The mechanisms underlying these effects are unclear. The resulting regional brain effects of cymba conchae stimulation observed in the healthy participants of this study provide a point of reference for understanding the mechanism underlying the effects of both invasive and non-invasive vagus nerve stimulation.

The anti-nociception effect is consistent with the present finding of cymba conchae stimulation-induced activation of periaqueductal gray, dorsal raphe, and locus coeruleus, each of which activates descending inhibitory pathways to the spinal cord dorsal horn [4,40].

The anti-depression effect is consistent with the activation of the amygdala [60] and may be boosted by nucleus accumbens activation, as depression has been shown to decrease the response of the nucleus accumbens to reward [49]. While Kraus et al. [35] and Dietrich et al. [11] reported deactivation of the amygdala and accumbens, respectively, using ear stimulation, they did not apply the stimulation to the cymba conchae; regional differential innervation of the ear may account for these different findings.

The anti-convulsion effect is consistent with the deactivation of the hippocampus [23,51]. In humans, temporal lobe epilepsy, with a focus in the hippocampus, is the most common form of drug-resistant epilepsy [47]. As the septum is a major source of neural input to the hippocampus [14,20], the septal activation, observed in response to cymba conchae stimulation in the present study, is a possible trigger for the observed hippocampal deactivation. Furthermore, the anterior thalamic activation is consistent with previous findings of fMRI and PET studies performed on patients with the implanted vagus nerve stimulator. In some cases, the increased thalamic activity was observed in the patients who were most responsive to vagus nerve stimulation [24,37,44]. In addition, the activation of the dorsal raphe and locus coeruleus found in the present study is consistent with the anticonvulsive effects of invasive vagus nerve stimulation and external ear stimulation [15,34,39].

Two noteworthy observations

Unexpected widespread activation of NTS by cymba conchae stimulation—

Contrary to expectation based on evidence of a viscerotopic organization of the NTS [1,54], the cymba conchae stimulation in the present study activated not just the rostral region of the NTS, but rather much of the rostrocaudal extent of the NTS through the medulla oblongata (Fig. 3a). This widespread activation is consistent with neuroanatomical evidence in cats of the afferent distribution of the auricular branch of the vagus nerve, i.e., more dispersed throughout the subnuclei of the NTS than viscerotopically distributed [45]. This convergent evidence indicates an extensive distribution of, and perhaps diverse role for, the auricular branch of the vagus. Furthermore, the widespread activation of the NTS in the present study is consistent with the widespread activation found on the primary somatosensory cortex (Fig. 8a,c), i.e., both somatosensory areas (e.g., face, head) and visceral areas (e.g., the visceral region of SI and the visceral genital region -- the paracentral lobule) were activated in response to cymba conchae stimulation. This activity was not observed in the earlobe

(control) stimulation condition, in which case discrete activity was found in the nucleus cuneatus and only somatosensory regions of the primary sensory cortex (Fig. 8b,c).

Activation of the paracentral lobule by cymba conchae stimulation—While this finding may at first seem anomalous (because the paracentral lobule contains the homuncular "genital sensory cortex"), there is actually convergent supportive evidence. We reported recently, based on fMRI, that vaginal, cervical, and clitoral self-stimulation activate overlapping regions of the paracentral lobule [33]. Previously, we reported evidence that the vagus nerves convey sensory activity from the vagina and cervix [32]. That is, using fMRI, we found that the NTS was activated in women with complete spinal cord injury at T10 and above, injury that would block all the known genito-spinal ascending pathways to the brain. The only likely remaining sensory innervation of the vagina and cervix is the vagus, for which there is evidence in rats [9,30,46]. Furthermore, the women with complete spinal cord injury cited above reported perceptual awareness of the vaginal and cervical stimulation, but not clitoral, trunk or limb awareness below the level of the injury. In that study, we also showed evidence of activation of the paracentral lobule in some of the cases. Thus, while it is surprising that in the present study we found vagal (visceral) activation of ("somatic") paracentral lobule in response to cymba conchae stimulation, our reported observations that the women with complete spinal cord injury at or above T10 [31,32] were aware of vaginal and cervical stimulation, which could only have been conveyed by the vagus sensory nerves, provides evidence that this vagal afferent activity can "rise" to the level of perceptual awareness.

Caveats

One could argue that the parameters selected for the analysis of the brainstem are insufficiently conservative. However, we are confident that the significant activation of the NTS and other brainstem nuclei are not false positives on the basis that the same analysis criteria applied to the control, earlobe, stimulation failed to reveal activation of NTS or its projections. Instead, in the control, earlobe stimulation condition, there was significant activation of the nucleus cuneatus, which receives sensory information conveyed by spinal nerves above the 6th thoracic vertebra, and thus, where the greater auricular nerve would project [14].

A potential limitation of this study is that cardiac and respiratory activities were not available for use as regressors in the analysis. While Clancy et al. [8] reported that stimulation of the tragus (partially innervated by ABVN [48]) increased heart rate variability, in the parameters used in the present study, which were much lower in intensity and duration, and applied to the cymba conchae (exclusively innervated by ABVN [48]), we found no significant effect on heart rate (unpublished data). In addition, in the present study, it is unlikely that these factors contributed to the activity elicited by cymba conchae stimulation, for they did not influence the fMRI response to the control, earlobe, stimulation.

Conclusion

The present findings provide fMRI evidence in humans that the ABVN, via the cymba conchae, projects to the NTS, which is the first central relay of vagal afferents, and to other

primary and higher-order vagal projections in the brainstem and forebrain. This non-invasive electrical stimulation of the “somatic” (i.e., external ear) afferent branch of the vagus nerve activates both “visceral” and “somatic” vagal projections in the brain. Furthermore, the patterns of activation and deactivation observed in the healthy participants of this study now provide a point of reference for understanding the mechanism(s) underlying the anti-convulsive, antidepressive, and antinociceptive effects of t-VNS and VNS. The present finding that brain sites to which the vagus projects remain active after cessation of the cymba conchae stimulation suggests that there may be a concomitant persistence of the cognitive and behavioral effects of the stimulation.

Acknowledgments

This study was supported by Cerbomed, GmbH (Erlangen, Germany) and by the National Institutes of Health Grant 2R25 GM 060826. We gratefully acknowledge the excellent assistance of Wendy Birbano, Dr. Nan Wise, Dr. Kachina Allen, and John Del’Italia in acquiring the fMRI data, and Kaily Paulino for recommending the control orientation of the stimulating electrodes.

References

1. Altschuler, SM.; Rinaman, L.; Miselis, RR. Viscerotopic representation of the alimentary tract in the dorsal and ventral vagal complexes in the rat. In: Ritter, S.; Ritter, RC.; Barnes, CD., editors. Neuroanatomy and Physiology of Abdominal Vagal Afferents. Boca Raton: CRC Press; 1992. p. 22-53.
2. Andersson, JLR.; Jenkinson, M.; Smith, SM. FMRIB technical report TR07JA1. 2007. Non-linear optimisation.
3. Andersson, JLR.; Jenkinson, M.; Smith, SM. FMRIB technical report TR07JA2. 2007. Non-linear registration, aka Spatial normalisation.
4. Basbaum AI, Fields HL. Endogenous pain control mechanisms: review and hypothesis. Ann Neurol. 1978; 4:451–62. [PubMed: 216303]
5. Berthoud HR, Neuhuber WL. Functional and chemical anatomy of the afferent vagal system. Auton Neurosci. 2000; 85:1–17. [PubMed: 11189015]
6. Bohning DE, Lomarev MP, Denslow S, Nahas Z, Shastri A, George MS. Feasibility of vagus nerve stimulation-synchronized blood oxygenation level-dependent functional MRI. Invest Radiol. 2001; 36(8):470–9. [PubMed: 11500598]
7. Busch V, Zeman F, Heckel A, Menne F, Ellrich J, Eichhammer P. The effect of transcutaneous vagus nerve stimulation on pain perception--an experimental study. Brain Stimul. 2013; 6:202–9. [PubMed: 22621941]
8. Clancy JA, Mary DA, Witte KK, Greenwood JP, Deuchars SA, Deuchars J. Non-invasive vagus nerve stimulation in healthy humans reduces sympathetic nerve activity. Brain Stimul. Epub 2014 Jul 16. 10.1016/j.brs.2014.07.031
9. Collins JJ, Lin CE, Berthoud HR, Papka RE. Vagal afferents from the uterus and cervix provide direct connections to the brainstem. Cell Tissue Res. 1999; 295:43–54. [PubMed: 9931352]
10. DeGiorgio CM, Schachter SC, Handforth A, Salinsky M, Thompson J, Uthman B, et al. Prospective long-term study of vagus nerve stimulation for the treatment of refractory seizures. Epilepsia. 2000; 41:1195–200. [PubMed: 10999559]
11. Dietrich S, Smith J, Scherzinger C, Hofmann-Preiss K, Freitag T, Eisenkolb A, et al. A novel transcutaneous vagus nerve stimulation leads to brainstem and cerebral activations measured by functional MRI. Biomed Tech (Berl). 2008; 53:104–11. [PubMed: 18601618]
12. Ellrich J. Transcutaneous Vagus Nerve Stimulation. Euro Neurol Rev. 2011; 6:2–4.
13. Fay T. Observations and results from intracranial section of glossopharyngeus and vagus nerves in man. J Neurol Psychopathol. 1927; 8:110–23. [PubMed: 21611246]

14. Felten, DL.; Jozefowicz, R. Netter's Atlas of Human Neuroscience. Teterboro, NJ: Icon Learning Systems LLC; 2003.
15. Fornai F, Ruffoli R, Giorgi FS, Paparelli A. The role of locus coeruleus in the antiepileptic activity induced by vagus nerve stimulation. Eur J Neurosci. 2011; 33:2169–78. [PubMed: 21535457]
16. Frangos, E.; Allen, K.; Wise, N.; Ellrich, J.; Birbano, W.; Komisaruk, BR. Activation of vagus projections in humans via electrical stimulation of the external ear: fMRI time course analysis. Poster presented at the annual meeting of the Society for Neuroscience; San Diego, CA. 2013.
17. Frangos, E.; Allen, K.; Wise, N.; Ellrich, J.; Birbano, W.; Komisaruk, BR. Persistent activation of vagus projections in humans after electrical stimulation of the external ear: fMRI evidence. Poster presented at the annual meeting of the North American Neuromodulation Society; Las Vegas, NV. 2013.
18. Frangos, E.; Ellrich, J.; Dell'Italia, J.; Wise, N.; Komisaruk, BR. Activation of human vagus nerve afferent projections via electrical stimulation of external ear: fMRI evidence. Poster presented at the annual meeting of the Society for Neuroscience; New Orleans, LA. 2012.
19. Gao XY, Rong P, Ben H, Liu K, Zhu B, Zhang S. Morphological and electrophysiological characterization of auricular branch of vagus nerve: Projections to the NTS in mediating cardiovascular inhibition evoked by the acupuncture-like stimulation. Abstr Soc Neurosci. 2010; 694:22/HHH45.
20. Gogolák G, Stumpf C, Petsche H, Sterc J. The firing pattern of septal neurons and the form of the hippocampal theta wave. Brain Res. 1968; 7:201–7. [PubMed: 5638867]
21. Greve DN, Fischl B. Accurate and robust brain image alignment using boundary-based registration. Neuroimage. 2009; 48:63–72. [PubMed: 19573611]
22. Hein E, Nowak M, Kiess O, Biermann T, Bayerlein K, Kornhuber J, et al. Auricular transcutaneous electrical nerve stimulation in depressed patients: a randomized controlled pilot study. J Neural Transm. 2013; 120:821–7. [PubMed: 23117749]
23. Henry TR, Bakay RA, Votaw JR, Pennell PB, Epstein CM, Faber TL, et al. Brain blood flow alterations induced by therapeutic vagus nerve stimulation in partial epilepsy: I. Acute effects at high and low levels of stimulation. Epilepsia. 1998; 39:983–90. [PubMed: 9738678]
24. Henry TR, Votaw JR, Pennell PB, Epstein CM, Bakay RAE, Faber TL, et al. Acute blood flow changes and efficacy of vagus nerve stimulation in partial epilepsy. Neurology. 1999; 52(6):1166–73. [PubMed: 10214738]
25. Jenkinson M, Bannister P, Brady M, Smith S. Improved optimisation for the robust and accurate linear registration and motion correction of brain images. NeuroImage. 2002; 17:825–41. [PubMed: 12377157]
26. Jenkinson M, Smith SM. A Global Optimisation Method for Robust Affine Registration of Brain Images. Med Image Anal. 2001; 5:143–56. [PubMed: 11516708]
27. Jenkinson M. A fast, automated, n-dimensional phase unwrapping algorithm. Magn Reson Med. 2003; 49:193–7. [PubMed: 12509838]
28. Jenkinson M. Improving the registration of B0-distorted EPI images using calculated cost function weights. Tenth Int Conf on Functional Mapping of the Human Brain. 2004
29. Kirchner A, Birklein F, Stefan H, Handwerker HO. Left vagus nerve stimulation suppresses experimentally induced pain. Neurology. 2000; 55:1167–71. [PubMed: 11071495]
30. Komisaruk BR, Bianca R, Sansone G, Gomez LE, Cueva-Rolon R, Beyer C, et al. Brain-mediated responses to vaginocervical stimulation in spinal cord-transected rats: Role of the vagus nerves. Brain Res. 1996; 708:128–34. [PubMed: 8720868]
31. Komisaruk BR, Gerdes CA, Whipple B. "Complete" spinal cord injury does not block perceptual responses to genital self-stimulation in women. Arch Neurol. 1997; 54:1513–20. [PubMed: 9400361]
32. Komisaruk BR, Whipple B, Crawford A, Liu WC, Kalnin A, Mosier K. Brain activation during vaginocervical self-stimulation and orgasm in women with complete spinal cord injury: fMRI evidence of mediation by the vagus nerves. Brain Res. 2004; 1024:77–88. [PubMed: 15451368]
33. Komisaruk BR, Wise N, Frangos E, Liu WC, Whipple B, Brody S. Women's clitoris, vagina and cervix mapped on the sensory cortex, using fMRI. J Sex Med. 2011; 8:2822–30. [PubMed: 21797981]

34. Krahl SE, Clark KB, Smith DC, Browning RA. Locus coeruleus lesions suppress the seizure-attenuating effects of vagus nerve stimulation. Epilepsia. 1998; 39:709–14. [PubMed: 9670898]
35. Kraus T, Hösl K, Kiess O, Schanze A, Kornhuber J, Forster C. BOLD fMRI deactivation of limbic and temporal brain structures and mood enhancing effect by transcutaneous vagus nerve stimulation. J Neural Transm. 2007; 114:1485–93. [PubMed: 17564758]
36. Kraus T, Kiess O, Hösl K, Terekhin P, Kornhuber J, Forster C. CNS BOLD fMRI effects of sham-controlled transcutaneous electrical nerve stimulation in the left outer auditory canal – A pilot study. Brain Stimul. 2013; 6(5):798–804. [PubMed: 23453934]
37. Liu WC, Mosier K, Kalnin AJ, Marks D. BOLD fMRI activation induced by vagus nerve stimulation in seizure patients. J Neurol Neurosurg Psychiatry. 2003; 74:811–3. [PubMed: 12754361]
38. Lomarev M, Denslow S, Nahas Z, Chae JH, George MS, Bohning DE. Vagus nerve stimulation (VNS) synchronized BOLD fMRI suggests that VNS in depressed adults has frequency/dose dependent effects. J Psychiatr Res. 2002; 36(4):219–27. [PubMed: 12191626]
39. Mazarati AM, Baldwin RA, Shinmei S, Sankar R. In vivo interaction between serotonin and galanin receptors types 1 and 2 in the dorsal raphe: implication for limbic seizures. J Neurochem. 2005; 95:1495–503. [PubMed: 16219029]
40. Millan MJ. Descending control of pain. Prog Neurobiol. 2002; 66:355–474. [PubMed: 12034378]
41. Nahas Z1, Teneback C, Chae JH, Mu Q, Molnar C, Kozel FA, Walker J, Anderson B, Koola J, Kose S, Lomarev M, Bohning DE, George MS. Serial vagus nerve stimulation functional MRI in treatment-resistant depression. Neuropsychopharmacology. 2007; 32(8):1649–60. [PubMed: 17203016]
42. Naidich, TP.; Duvernoy, HM.; Delman, BN.; Sorensen, AG.; Kollias, SS.; Haacke, EM. Duvernoy's Atlas of the Human Brain Stem and Cerebellum. Vienna: Springer-Verlag/Wien; 2009.
43. Napadow V, Edwards RR, Cahalan CM, Mensing G, Greenbaum S, Valovska A, et al. Evoked pain analgesia in chronic pelvic pain patients using respiratory-gated auricular vagal afferent nerve stimulation. Pain Med. 2012; 13:777–89. [PubMed: 22568773]
44. Narayanan JT, Watts R, Haddad N, Labar DR, Li PM, Filippi CG. Cerebral activation during vagus nerve stimulation: a functional MR study. Epilepsia. 2002; 43(12):1509–14. [PubMed: 12460253]
45. Nomura S, Mizuno N. Central distribution of primary afferent fibers in the Arnold's nerve (the auricular branch of the vagus nerve): a transganglionic HRP study in the cat. Brain Res. 1984; 292:199–205. [PubMed: 6692153]
46. Ortega-Villalobos M, García-Bazán M, Solano-Flores LP, Ninomiya-Alarcón JG, Guevara-Guzmán R, Wayner MJ. Vagus nerve afferent and efferent innervation of the rat uterus: an electrophysiological and HRP study. Brain Res Bull. 1990; 25:365–71. [PubMed: 2292033]
47. Panayiotopoulos, CP. Chipping Norton. Oxfordshire, UK: Bladon Medical Publishing; 2004. The Epilepsies: Seizures, Syndromes and Management.
48. Peuker ET, Filler TJ. The Nerve Supply of the Human Auricle. Clin Anat. 2002; 15:35–7. [PubMed: 11835542]
49. Pizzagalli DA, Holmes AJ, Dillon DG, Goetz EL, Birk JL, Bogdan R, et al. Reduced caudate and nucleus accumbens response to rewards in unmedicated individuals with major depressive disorder. Am J Psychiatry. 2009; 166:702–10. [PubMed: 19411368]
50. Poldrack, RA.; Mumford, JA.; Nichols, TE. Handbook of functional MRI data analysis. New York: Cambridge University Press; 2011.
51. Raedt R, Clinckers R, Mollet L, Vonck K, El Tahry R, Wyckhuys T, et al. Increased hippocampal noradrenaline is a biomarker for efficacy of vagus nerve stimulation in a limbic seizure model. J Neurochem. 2011; 117:461–9. [PubMed: 21323924]
52. Ruggiero DA, Underwood MD, Mann JJ, Anwar M, Arango V. The human nucleus of the solitary tract: visceral pathways revealed with an "in vitro" postmortem tracing method. J Auton Nerv Syst. 2000; 79:181–90. [PubMed: 10699650]

53. Rush AJ, George MS, Sackeim HA, Marangell LB, Husain MM, Giller C, Nahas Z, Haines S, Simpson RK Jr, Goodman R. Vagus nerve stimulation (VNS) for treatment-resistant depressions: a multicenter study. Biol Psychiatry. 2000; 47:276–286. [PubMed: 10686262]

54. Sawchenko PE. Central connections of the sensory and motor nuclei of the vagus nerve. J Auton Nerv Syst. 1983; 9:13–26. [PubMed: 6319474]

55. Stefan H, Kreiselmeyer G, Kerling F, Kurzbuch K, Rauch C, Heers M, et al. Transcutaneous vagus nerve stimulation (t-VNS) in pharmacoresistant epilepsies: a proof of concept trial. Epilepsia. 2012; 53:e115–8. [PubMed: 22554199]

56. Tekdemir I, Aslan A, Elhan. A clinico-anatomic study of the auricular branch of the vagus nerve and Arnold's ear-cough reflex. Surg Radiol Anat. 1998; 20:253–7. [PubMed: 9787391]

57. The Vagus Nerve Stimulation Study Group. A randomized controlled trial of chronic vagus nerve stimulation for treatment of medically intractable seizures. Neurology. 1995; 45:224–30. [PubMed: 7854516]

58. Wetzel B, Pavlovic D, Kuse R, Gibb A, Merk H, Lehmann C, et al. The effect of auricular acupuncture on fentanyl requirement during hip arthroplasty: a randomized controlled trial. Clin J Pain. 2011; 27:262–7. [PubMed: 21346689]

59. Woolrich MW, Ripley BD, Brady JM, Smith SM. Temporal Autocorrelation in Univariate Linear Modelling of FMRI Data. NeuroImage. 2001; 14:1370–86. [PubMed: 11707093]

60. Young KD, Zotev V, Phillips R, Misaki M, Yuan H, Drevets WC, Bodurka J. Real-time FMRI neurofeedback training of amygdala activity in patients with major depressive disorder. PLoS One. 2014; 9:e88785. [PubMed: 24523939]

Highlights

The present study provides fMRI evidence in humans that mild electrical stimulation of the external ear in the region of the cymba conchae activates the main visceral sensory nucleus of the vagus nerve – the nucleus of the solitary tract.

Cymba conchae stimulation also activated classical central projections of the vagus nerve through out the brainstem and forebrain, including a widespread region of the sensory cortex.

The patterns of activation and deactivation observed in the healthy participants of this study provide a point of reference for understanding the mechanism(s) underlying the anti-convulsive, antidepressive, and antinociceptive effects of t-VNS and VNS.

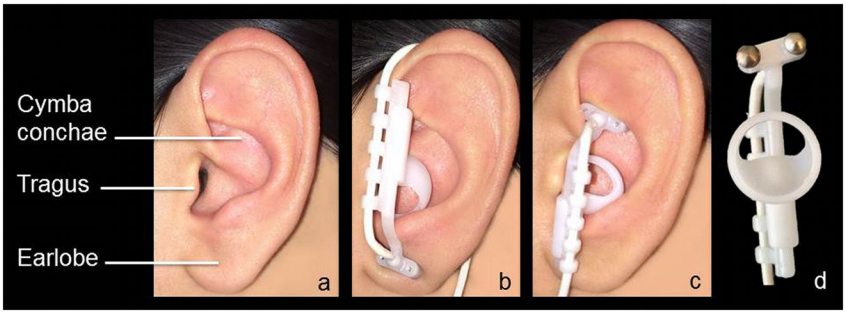

Figure 1.

a. The left external ear indicating the regions referred to in the Introduction and Stimulation Procedure section; b. Position of the earpiece during the control condition (earlobe stimulation); c. Position of the earpiece during the experimental condition (cymba conchae stimulation); d. Detail of the earpiece and the pair of titanium electrodes.

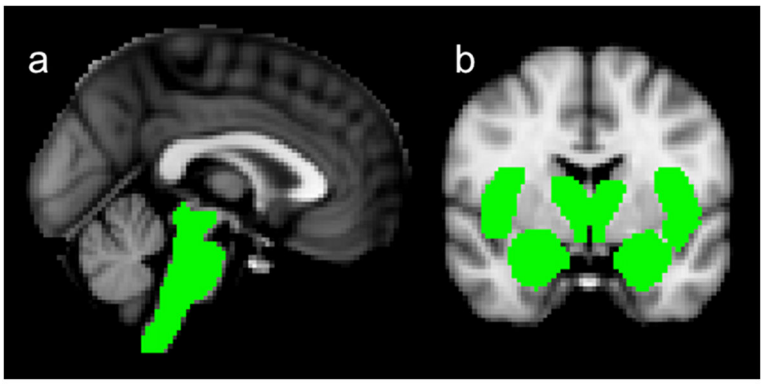

Figure 2.

Selected vagal projections (“masked” in green) for the ROI analyses designed to test the hypothesis. a. Mask for the brainstem analysis. b. Masks for the forebrain analysis: thalamus, hypothalamus, amygdala, nucleus accumbens, insula (pictured in coronal slice), and (included but not pictured in coronal slice) paracentral lobule and hippocampus.

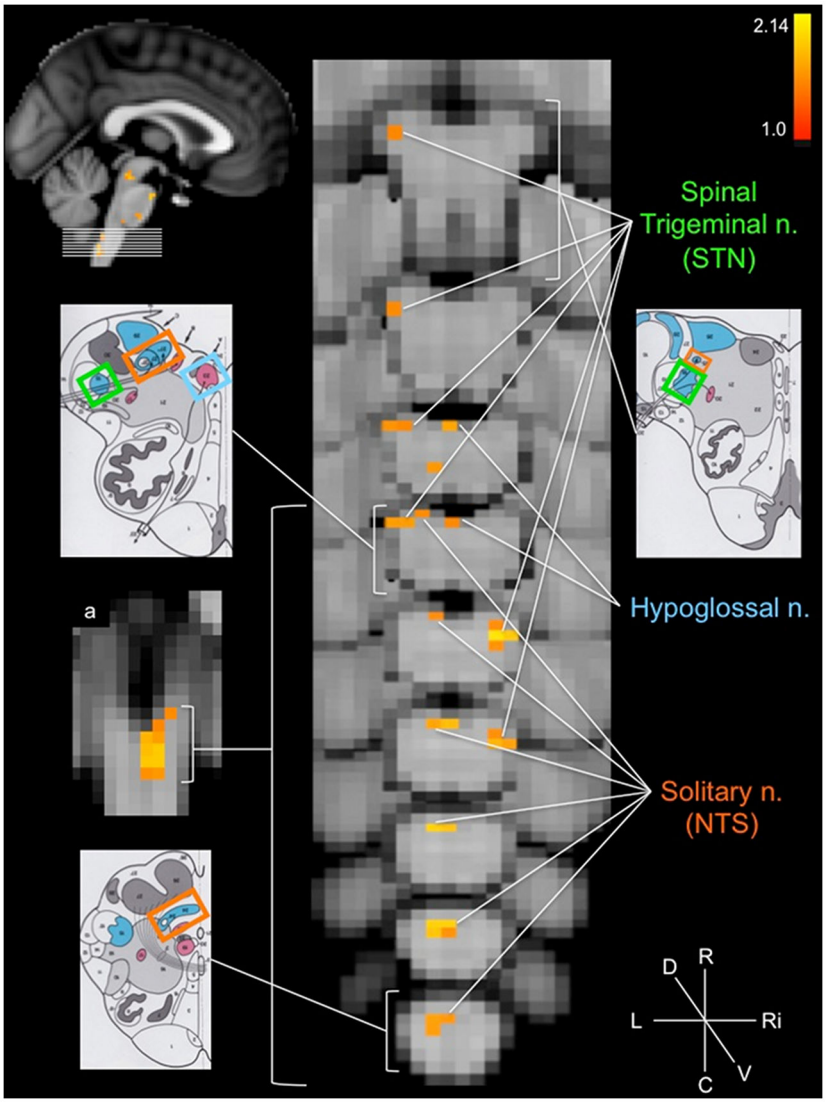

Figure 3.

Medulla oblongata activations: cymba conchae > earlobe. Serial axial slices (location indicated by top left sagittal image, MNI152 z-coordinates: z = 4–12) showing the regions that were significantly active during cymba conchae stimulation compared to earlobe (control) stimulation. The left schematic diagrams from the Naidich et al. [42] atlas indicate the location of the corresponding labeled nuclei. Color-coding: solitary nucleus = orange; hypoglossal nucleus = blue; spinal trigeminal nucleus = green. Compass: R = rostral; C = caudal; L = left; Ri = right; D = dorsal; V = ventral. a. Coronal section indicating widespread left (ipsilateral) NTS activation. This and all the following figures are based upon group data, N=12. Top right colored bar indicates the z-score range. The z-score convention is the same for all the following figures.

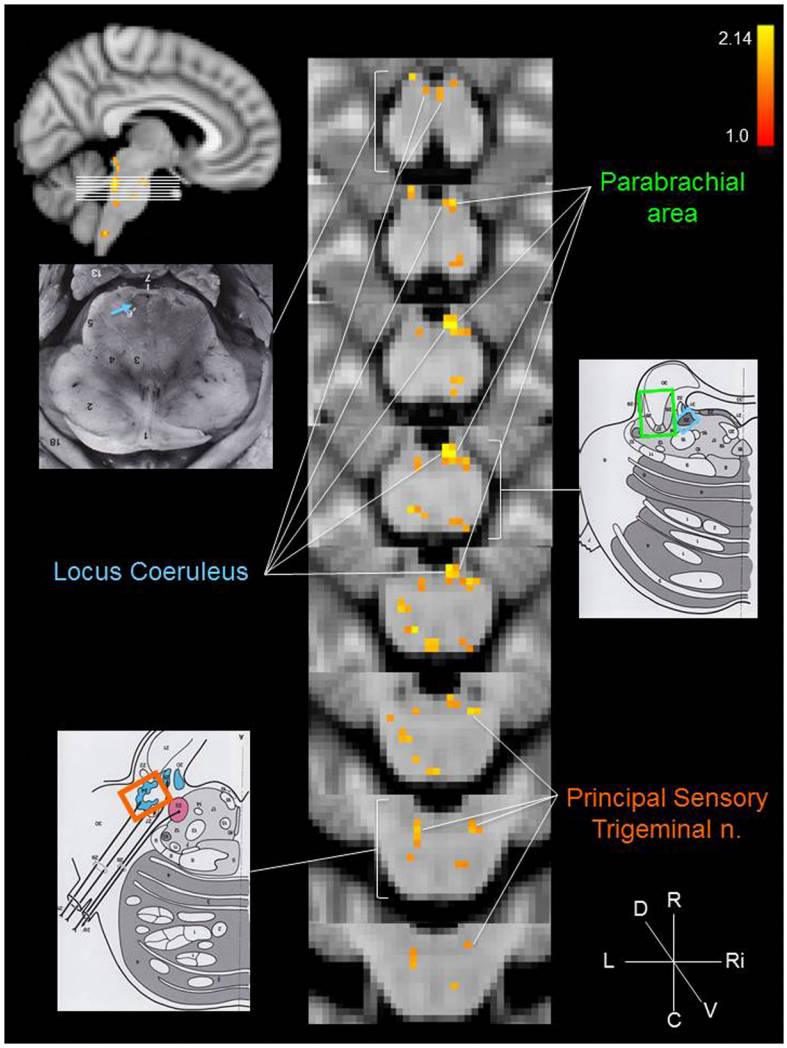

Figure 4.

Pons and lower midbrain activations: cymba conchae > earlobe. Conventions are the same as in Figure 2 with the exception of the color-coding: principal sensory trigeminal nucleus = orange; locus coeruleus = blue; parabrachial area = green. MNI152 z-coordinates: z = 19–26.

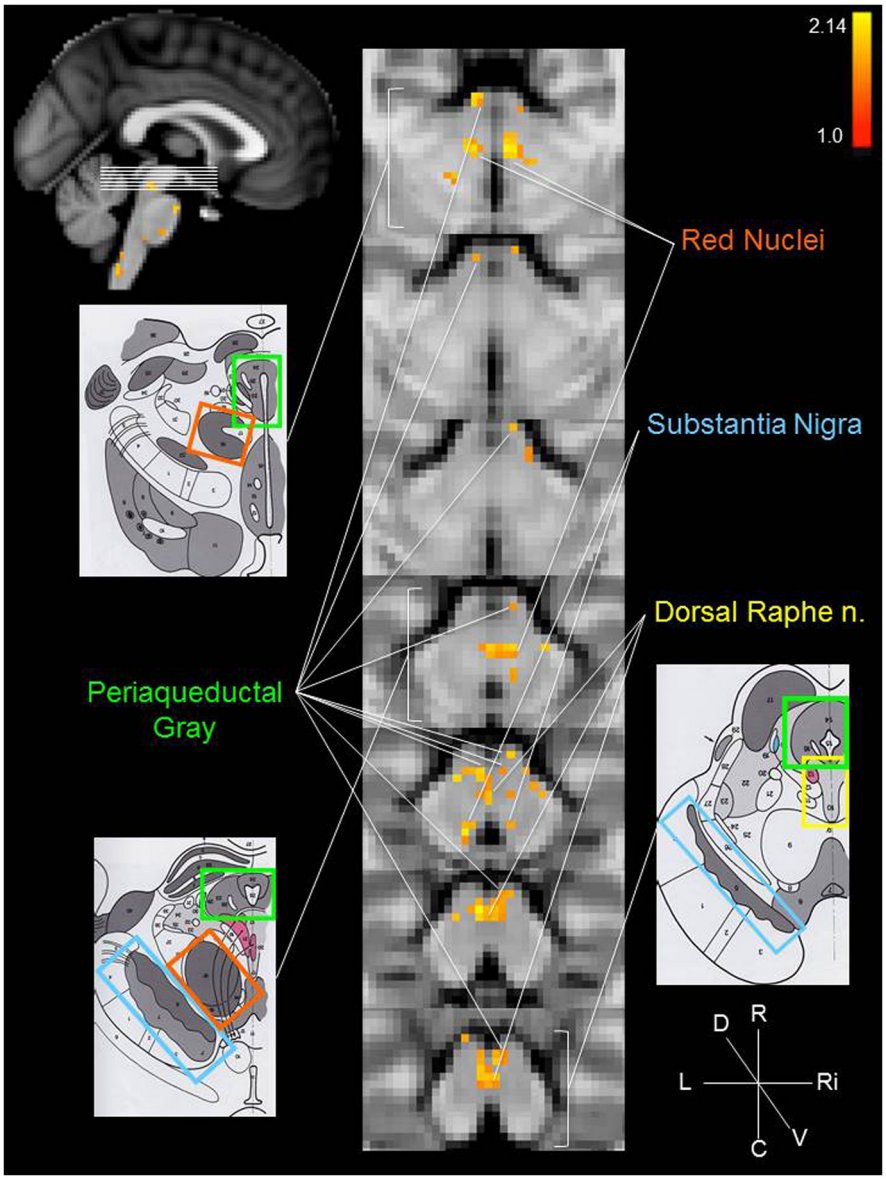

Figure 5.

Midbrain activations: cymba conchae > earlobe. Conventions are the same as in Figure 2 with the exception of the color-coding: red nuclei = orange; substantia nigra = blue; dorsal raphe nuclei = yellow; periaqueductal gray = green. MNI152 z-coordinates: z = 27–33.

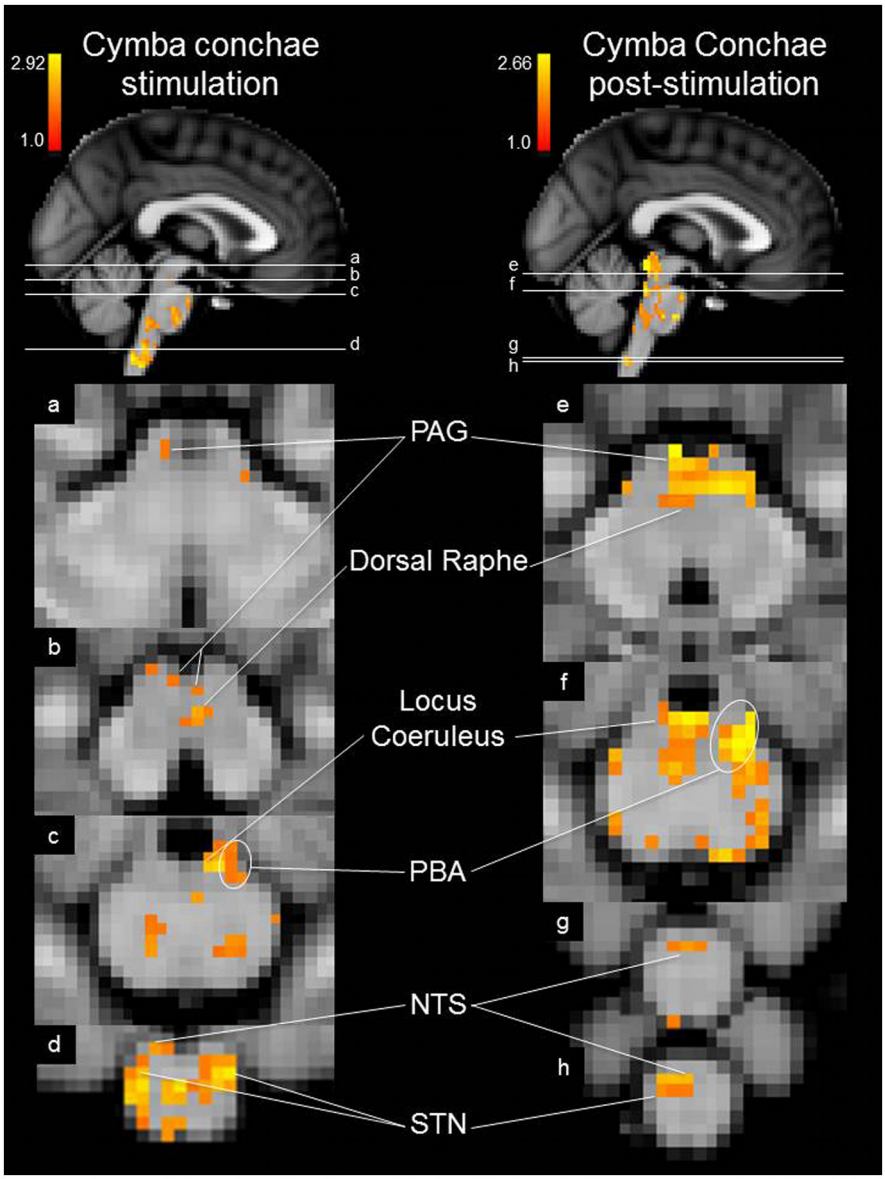

Figure 6.

Mean effects of cymba conchae stimulation and post-stimulation in the brainstem. Labeled regions were each significantly activated. MNI152 z-coordinates: a. z = 31, b. z = 27, c. z = 23, d. z = 8, e. z = 29, f. z = 24, g. z = 6, h. z = 5.

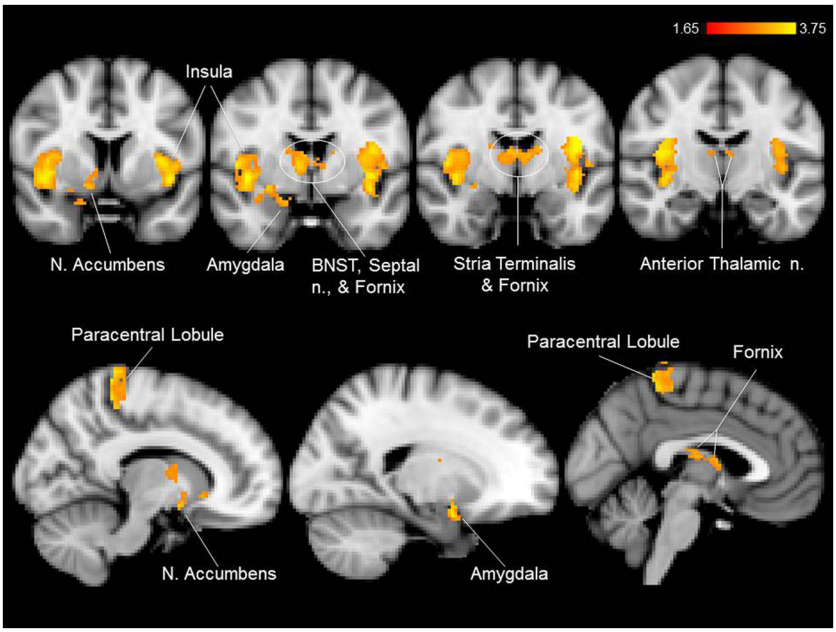

Figure 7.
Mean effects of cymba conchae stimulation in the forebrain. Labeled regions were each significantly activated.

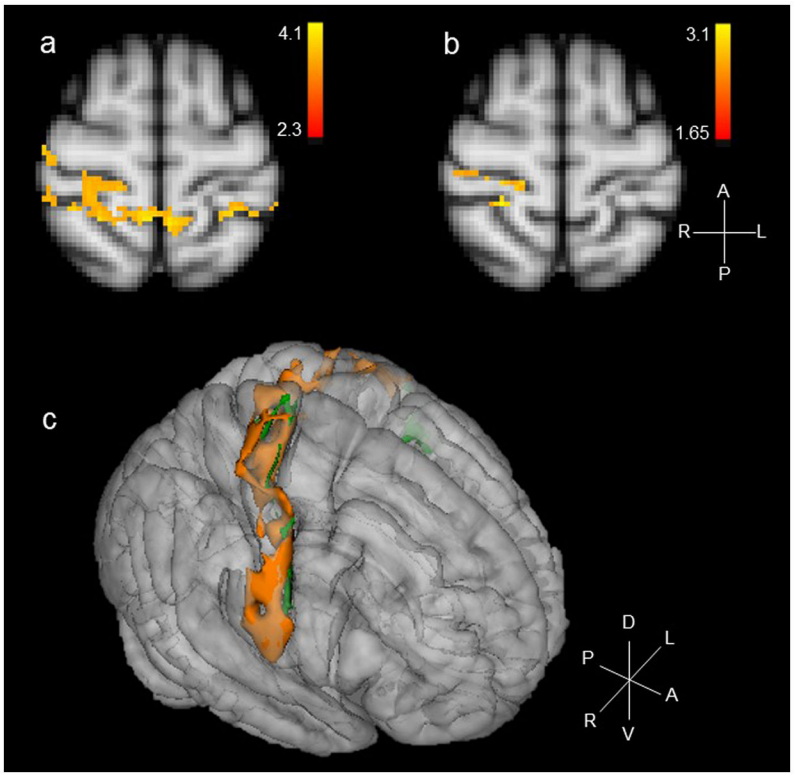

Figure 8.

a. Mean effects of cymba conchae stimulation on the primary somatosensory cortex; b. Mean effects of earlobe (control) stimulation on the primary somatosensory cortex; c. Three-dimensional composite of the sensory cortical response to stimulation of cymba conchae (orange) and earlobe (green). Compass: R = right; L = left; A = anterior; P = posterior; D = dorsal; V = ventral.

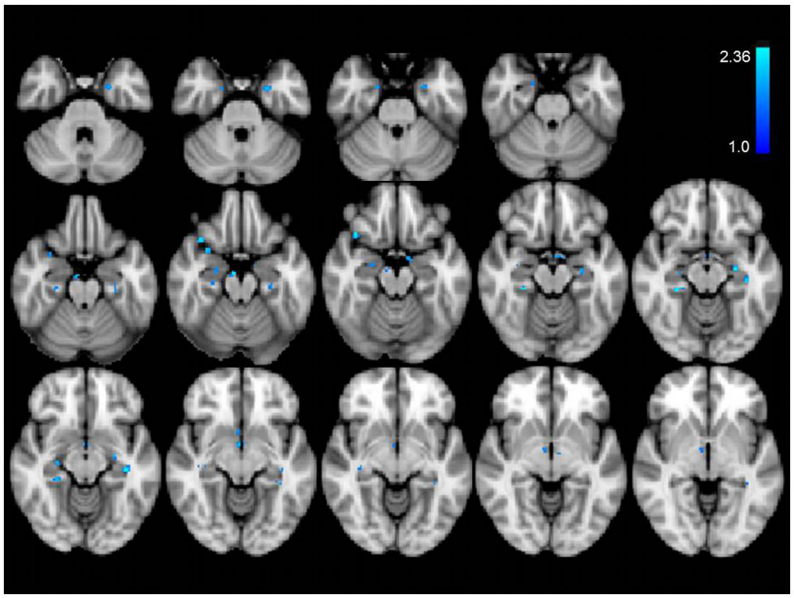

Figure 9.

Significant deactivations of cymba conchae stimulation. Note the deactivation sites dispersed in hippocampus and parahippocampal gyrus. Deactivation occurred also in hypothalamus.

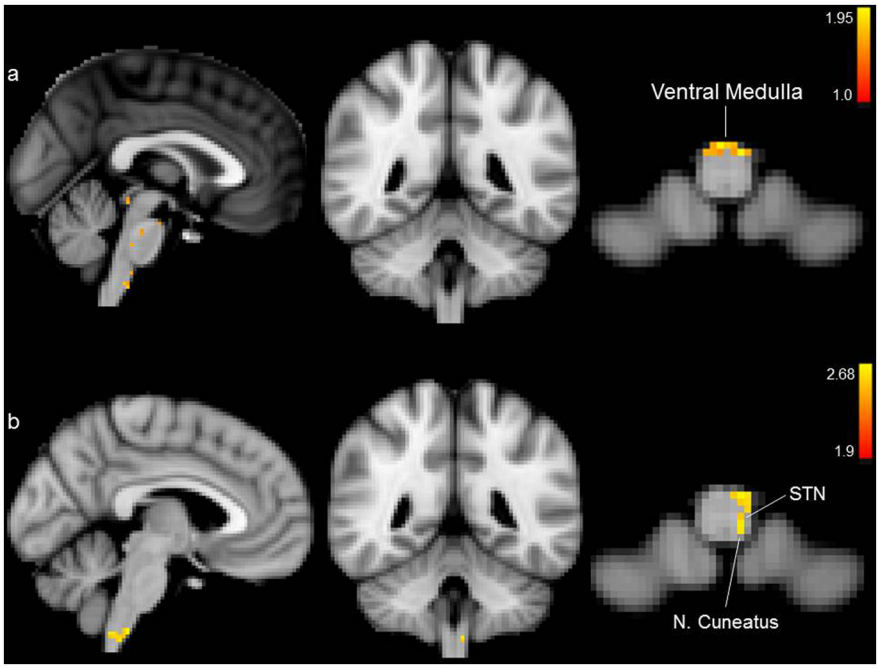

Figure 10.

Brainstem activations for the control condition. a. Earlobe (control) stimulation > cymba conchae stimulation; b. Mean effects of earlobe (control) stimulation. Activations were significant only in the regions of the medulla oblongata that are labeled. We found no evidence of significant activation of solitary nucleus or its projections. MNI152 z-coordinates: a. and b. z = 6.

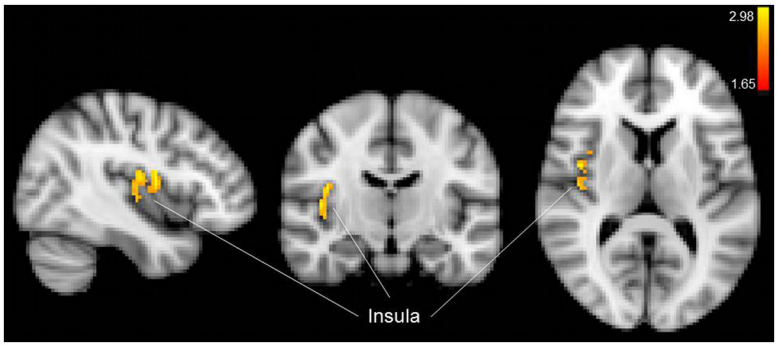

Figure 11.
Mean effects of earlobe (control) stimulation in the forebrain.

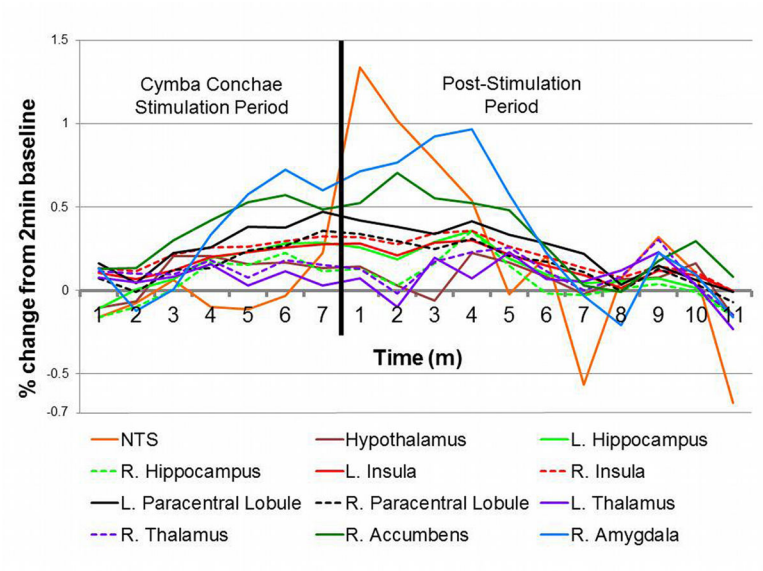

Figure 12.

Time-course analysis of the percent change of the BOLD signal for each significantly active region compared to the initial 2 minutes of rest (baseline). Note the gradual increase in activity during the 7 minutes of cymba conchae stimulation. For most regions, the activity peaked then persisted after cessation of the stimulation.

Table 1

Clusterwise corrected p-values for ROI and Whole-brain analyses. (n = 12)

	CC > BL				E(C) > BL		CC > E(C)		E(C) > CC		CC post-stimulation			
	ROI		Whole brain		ROI	Whole brain	ROI	Whole brain	ROI	Whole brain	ROI		Whole brain	
	↑	↓	↑	↓	↑	↑	↑	↑	↑	↑	↑	↓	↑	↓
Brainstem			◆			◆		◆		◆			◆	
dorsal raphe	b***	u		u	u		b***		u		b***	u		u
hypoglossal	l***	u		u	u		l***		u		l***	u		u
locus coeruleus	b***	u		u	u		b***		u		b***	u		u
nucleus cuneatus	u	u		u	l**		u		u		u	u		u
parabrachial area	r***	u		u	u		r***		u		r***	u		u
periaqueductal gray	b***	u		u	u		b***		u		b***	u		u
principal spinal trigeminal nucleus	b***	u		u	u		b***		u		u	u		u
red nucleus	b***	u		u	u		b***		u		b***	u		u
solitary nucleus	l***	u		u	u		l***		u		l***	u		u
spinal trigeminal nucleus	b***	u		u	l**		b***		u		l***	u		u
substantia nigra	b***	u		u	u		b***		u		b***	u		u
ventral medulla	b***	u		u	l**		u		b***		u	u		u
Forebrain														
amygdala	r***	u	r***	u	u	u	r***	r***	u	u	r***	u	u	u
anterior cingulate	ni	ni	b***	u	ni	u	ni	b***	ni	u	ni	ni	u	b**
bed nucleus of the stria terminalis	b***	u	b***	u	u	u	b***	b***	u	u	u	u	u	u
caudate	ni	ni	r***	u	ni	u	ni	u	ni	u	ni	ni	l***	u
cerebellum	ni	ni	b***	u	ni	r**	ni	b***	ni	u	ni	ni	b**	u
fornix	b***	u	b***	u	u	u	b***	b***	u	u	u	u	u	u
hippocampus	u	b***	u	b***	u	u	u	u	u	u	b***	u	l***	u
hypothalamus	u	b***	u	b***	u	u	u	u	u	u	u	u	u	u
insula	b***	u	b***	u	r*	r***	b***	b***	u	u	b***	u	r***	u

	CC > BL				E(C) > BL		CC > E(C)		E(C) > CC		CC post-stimulation			
	ROI		Whole brain		ROI	Whole brain	ROI	Whole brain	ROI	Whole brain	ROI		Whole brain	
	↑	↓	↑	↓	↑	↑	↑	↑	↑	↑	↑	↓	↑	↓
nucleus accumbens	r***	u	b***	u	u	u	r***	r***	u	u	l***	r***	u	u
orbital frontal cortex	ni	ni	b***	u	ni	u	ni	r*	ni	u	ni	ni	u	u
paracentral lobule	b*	u	b***	u	u	u	b***	b***	u	u	u	b***	u	b**
postcentral gyrus	b***	u	b***	u	b*	u	b*	b***	u	u	u	u	u	b**
putamen	ni	ni	r***	u	ni	u	ni	u	ni	u	ni	ni	r***	u
stria terminalis	b***	u	b***	u	u	u	b***	b***	u	u	u	u	u	u
	1													
thalamus	b***	u	b***	u	u	u	b***	b***	u	u	b***	u	b**	u

CC = cymba conchae stimulation

E(C) = earlobe (control) stimulation

BL = baseline

◆ = Widespread activity throughout brainstem (corrected, p<0.0001)

1 bilateral thalamic activations found specifically within anterior thalamic nuclei

↑ = activation

↓= deactivation

* = p < 0.04

** = p < 0.01

*** = p < 0.0001

r = right

l = left

b = bilateral

u = undetected

ni = region not included in ROI analysis